International Journal of
INTELLIGENT SYSTEMS AND APPLICATIONS IN ENGINEERING
ISSN:2147-6799 www.ijisae.org Original Research Paper

Complete Employment of Every Potentiality for the Optimal Detection of Alzheimer

S. Beatrice and Janaki Meena.M

Submitted: 07/02/2024 **Revised**: 15/03/2024 **Accepted**: 21/03/2024

Abstract: The main intention of this paper is to detect Alzheimer disease from the input MRI image based on deep learning methods. To effectively eliminate this Alzheimer's disease, an analytic tool becomes mandatory that is very cost-effective, readily available, and more efficient, which senses dementia much earlier before dementia becomes Alzheimer's. To overcome this drawback, this uses deep learning methods to detect Alzheimer disease. Knowledge of Alzheimer disease is gained through an offline process. The adaptive bilateral filter clears the noise in the input brain image in the online procedure, and then histogram equalization improves contrast. Then these images are used to find the Alzheimer-affected area. The artificial bee colony segmentation method is used to find the Alzheimer area. The gaps in Alzheimer's area are filled with the use of the ABC segmented image's mathematical morphology method. The textural characteristics are then utilized to detect Alzheimer's disease. After the location of Alzheimer's disease is found, the next step is to identify the severity of the disease by extracting its features. This study utilizes six extraction approaches, including the local binary pattern, histogram of gradients, SIFT, transformational wavelet features, and the Zernike moment. The BeePCNN algorithm is employed for the selection of the most excellent feature after the extraction of the features. These features are finally categorized using a deep learning method named FGPCNN. To analyze the performance of the proposed approach, this work uses real-time MRI datasets. The proposed technique provides 99.23 accuracy, the sensitivity value is 99.31, and the output value is the specific value and the error rate. The pooling layer in a convolutional neural network (CNN) is commonly used to down-sample the feature maps, reducing their spatial dimensions while preserving important features. Two types of pooling layers exist: maximum pooling and average pooling. The value of the biggest pixel in the receptive field of the filter is evaluated during max pooling. On average, the average of all values in the receptive field is evaluated. The pooling layer output is provided as an input to the following convolution layer. For big maps, CNN has extremely high computer costs. CNN trains big maps slowly. To overcome the disadvantages of the above, the Fuzzy Genetic Pulse Coupled Neural Network (FGPCNN) optimization technique is proposed.

Keywords *Alzheimer detection, PSO, ABC, BeePCNN, GA, CNN, FGPCNN.*

1. Introduction

Accelerate degeneration and dying of Brain cell connections, which would sooner or later turn out to be the reason for an irreversible, continual ailment in the brain, and can bit by bit devastate the logical and reasoning ability by making the subject incapable of responding promptly to a simple conversation or even to carry out a simple task on their own is termed to be Alzheimer. One century has passed after discovering Alzheimer's disease, but apt therapy to cure Alzheimer's disease remains an unsolved puzzle. The most menacing harm posed by Alzheimer's hallucination is that the effect gets compounded with time. The antecedent mild memory loss can even end up annoying an individual's level to an acute extent. The individual becomes just incapable of engaging in a simple conversation and behave accordingly.

To effectively eliminate this Alzheimer's disease, an analytic tool becomes mandatory that is very cost-effective, becomes readily available, and is more efficient, which senses dementia much earlier before dementia becomes Alzheimer's. The development of such a useful analytic tool or analytic algorithm vitally requires analyzing the pros and cons of the methodologies suggested for automated analysis of disease and emerging with the best algorithm enriched with precision, Specificity, and Accuracy. Yep, the evaluation of a hybridized optimal algorithm is accomplished through a series of Hybridized optimal approaches.

In general, the image fusion process is the name given to the process that gathers and encompasses all the essential information from numerous images into a single one. This single fused image is more accurate and precise than any single source image and is got by the integration of all the information required. The image fusion process reduces data. It also enables the construction of more appropriate and understandable images for humans and machines' perception. The resulting image is found to be more insightful than all the input data.

Data reduction and image construction that upholds a large amount of information. The image becomes more appropriate and understandable for both computer and human perception and augments medical images' clinical

School of Computer Science and Engineering Department; Vellore Institute of Technology, Chennai-600127
Corresponding author: Janaki Meena.M (e-mail: janakimeena.m@vit.ac.in)

applicability. Any image fusion method is generally a combo of two phases: image registration and image fusion. As for as image registration is concerned, a special method is needed to fix the spatial relation between the various sets of images that frequently comprise unevenness reimbursement due to scale changes, rot, and translations. Whereas the image fusion primarily focuses on aptly identifying and selecting features that become more compatible with clinical assessment.

2. Related work

While focusing on an image the aspects considering aspects of the axial, coronal & sagittal plane, are taken into consideration. Several segmentation techniques have been analyzed to improve the classification accuracy and after thorough analysis, factor atrophy for segmentation using the Watershed algorithm is proposed for segmentation. For researchers, early detection of Alzheimer's is a troubling task. The SCNN (Siamese CNN) model for classifying the stages of dementia [1] have been developed, and the relevant extended approaches enable the extension of the work. The reduction of overlay was achieved, the maximum likelihood of the model effect was maximized and the accuracy of 99.05% was obtained while using OASIS data set.

Analysis was carried out using numerous feature extraction methods such as volume plus demographic, VBM volume plus Affine coefficients, Spatial texture, VOI intensity, frequency filter spatial, and DWT. After analysis, DWT, Spatial, Slantlet, and DCT features are used as input to ANN to classify Dementia. MCI is referred as Mild cognitive deficit for elderly people and it's not referred as dementia. MRI data has been used for MCI to AD conversion prediction. The CNN and Free surfer features, were brought together so as to have additional dimensional reduction and a sparse selection of features was done by using PCA and Lasso, that in turn resulted in a vector of features. Finally, the validation of the left-out cross is used to evaluate the approach's performance and an accuracy of 81.4% is achieved and an AUC of 87.8%[4] is got. Various biomarkers are employed in the diagnosis of AD and MCI. Combining three modalities MRI, FDG-PET, and CSF, by using the kernel combination method, 93.2% accuracy is achieved to classify AD and normal controls. But the multimodal classification was compared with the procedures using each modality. Serge Gauthier suggested the application of combining the grouped biomarkers [2] for the analysis amyloid deposition, pathological tau, neuro degeneration, termed it as ATN criteria, and added neuroimaging and biofluids, Cerebrospinal fluid. Freddle et al., combined amyloid with other biomarkers to stage progression. To detect AD, the features which are extracted from MRI can be measured by using the below methods 1. Voxel- based 2. Vertex based 3. Predefined ROI based. Volumes of brain matter (Specifically grey matter), white matter, and CSF are measured by voxel-based method. Cortical thickness measure is measured by vertex based and volume of specific regions such as hippocampus, amygdala, and entorhinal cortex are measured by ROI based features.

Dan jin et al., used attention-based networks and suggested a 3D attention network (3DAN) [6] that assimilates a RNN attenuation mechanism to mechanically arrest the most discriminatory locations in brain images and optimize feature extraction jointly. Finally, the performance of MRI images is shown.

The authors presented a new Prediction Model, which includes selecting the Random Forest (RF) ROI and GRU. Experiments show that their methodology achieves greater classification accuracy, and the prediction of early onset AD can be facilitated compared to existing algorithms. Their examination allows the identification of disease related brain regions across various image modalities.

Basheera et al. suggested an approach to extract grey matter voxels[7,8] of the brain and use CNN to classify it. The skull stripping algorithm removes unrelated tissues. Then, such segmented voxels are applied through hybrid independent component analysis. As a CNN input, segmented grey matter is used and achieves 90.47% accuracy.

A novel DL method called MKSCDDL was familiarized this study with the earlier effective outcome for face recognition uniting florbetapir-PET, sMRI, and FDG-PET classify AD, MCI, and cognitively unimpaired (CU). The findings indicated that MKSCDDL is performed better with neuro-imaging data for the classification and diagnosis of diseases.

To classify different levels of AD, a 3D-CNN style is built using a Support vector machine classifier. The multi class classification allows the three disease levels to be detected with the same algorithm. This algorithm increases the potential for the early detection of the illness. Therefore, this method was not possible with binary classification algorithms for diagnosing and predicting the disease. The condition's most desirable and discriminating generic characteristics were learned by Cascaded 3D-CNN, leading to high efficiency. The same architecture training results in less misclassification into standard controls with AD and MCI datasets, ensuring that no ill person is unidentified, which is essential for computerized diagnosis. 97.77 percent of precision is achieved by the proposed method.

The correlation grey level co-occurrence matrix is used to create the features. To improve the classification accuracy, clinical features are added. Multi class

classification is used where three classes are considered, namely NC, MCI, AD, and 79.8 percent accuracy is achieved in this classification, which is significant since the classes are highly similar. Compared to binary classification techniques, they achieved better results on multi class classification.

Farooq et al., proposed a 4-way classifier used to categorize AD, MCI, LMCI, and healthy controls. MRI scanned images are passed through skull stripping and gray matter segmentation and applied Deep convolutional neural networks to diagnose AD, LMCI, MCI, and healthy people by considering the ADNI dataset. Classification performance is improved.

3. Methodology

The common structural design for the detection of Alzheimer's disease has been presented in [Figure 1]. The knowledge of Alzheimer disease is gained in offline process. In Online procedure, noise in the input brain image is cleared with the adaptive bilateral filter followed by the contrast improvement process through histogram equalization. Then these images are used to find the Alzheimer affected area. The artificial bee colony segmentation method is used to find the Alzheimer area. The gaps in Alzheimer's area are filled with the use of the ABC segmented image's mathematical morphology method. The textural characteristics are then utilized to detect the Alzheimer's disease. After the location of the Alzheimer is found, the next step is to identify the severity of the Alzheimer's disease by extracting the features. This study utilizes six extraction approaches including the local binary pattern, histogram of gradients, SIFT, the transformation wavelet features, Zernike Moment. The Bee Pulse Coupled Neural Networks (BeePCNN) algorithm is employed for the selection of the most excellent feature after extraction of the features. These features are finally categorized utilizing deep learning methods.

3.1 Pre-processing (Noise Removal & Contrast Improvement)

The color value of the images is improved with the Histogram Equalization (HE) method in the pre-processing stage which is shown in [Figure 2].

HE is used to modifying image intensity to increase contrast as indicated in Eqn (1). Assume P_T is a brain image and by color values of particular position of P varies from 0 to 256. Assume T indicates the equalized histogram of image P for the color value available.

$$P_T = \frac{(\textit{Number of pixels with available intensity } n)}{(\textit{Total number of pixels})} \quad (1)$$

Where t = 0, 1. . . 255.

The image color value is recovered locally by splitting the input into several small regions and altering each region's color values to complete independently with a defined goal histogram. The improved results are shown in [Figure 3].

Next, Adaptive Bilateral Filter (ABF) [3] is utilized for on improved images for . ABF is a classic bilateral filter expansion. ABF includes several significant changes over bilateral ones. Locally adaptable range filters used in ABF. The range filter on the histogram is moved as indicated in (2) by adding a counterweight to the range filter.

$$ABF_{x_0,y_0} = \sum_{x=x_0-N}^{x_0+N}\sum_{y=y_0-N}^{y_0+N} exp\left(-\frac{(x-x_0)^2+(y-y_0)^2}{2\nabla_d^2}\right) X \quad (2)$$

$$exp\left(-\frac{(G[x_0,y_0]-G[x_0,y_0]-\delta[x_0,y_0])^2}{2\nabla_r^2[x_0,y_0]}\right)$$

Where x_0 sets the current pixel row index, $y_0$sets the current image pixel column index. x specifies the neighboring pixel row index. Y specifies the neighboring pixel column index. N is an adjacent window size. Ω_{x_0,y_0} is the center pixel of the nearby window[4].

The ABF degenerates into a typical bilateral filter if ∇_r and δ is fixed.

The mixture of local adaptive and global filters transforms ABF into a considerably more strong, smooth and crisp filter. In addition, the δ is calculated by Eqn (3).

$$\delta[x_0,y_0] = \begin{cases} MAXIMUM\left(\beta_{x_0,y_0}\right) - G[x_0,y_0], & if\ \Omega_{x_0,y_0} > 0 \\ MINIMUM\left(\beta_{x_0,y_0}\right) - G[x_0,y_0], & if\ \Omega_{x_0,y_0} < 0 \\ 0, & if\ \Omega_{x_0,y_0} = 0 \end{cases} \quad (3)$$

Some noises are normally surrounded with image Data throughout the image collection process that help to identify nodules. Noise may also be observed as nodules of disturbance. Therefore, additional noises have to be eliminated to identify the disease accurately. This ABF sharpens the picture by increasing the edge slope without overrunning. It may smooth the noise while increasing the image's edges and textures.

As demonstrated in [Figure 4], ABF offers excellent results compared to traditional filters such as medium filters. Problems with traditional filters, such overshooting, are emphasized by ABF and produce unpleasant ringing or halo objects.

ABF raises the edge slope without overlaying the picture and undershooting that makes the edges clean, sharp and non-artifact and also improves the overall look. Bilateral filter fails to restore a deteriorated image's sharpness. ABF gives excellent results both for improving sharpness and for removing noise as demonstrated in [Figure 4].

3.2 Segmentation

The segmentation method locates items or boundaries in the pre-processed image that contribute to the image area of interest. The picture is divided into segments to identify relevant information. In the Alzheimer disorder categorization, the disorder nodule from the pre-processed image needs to be segmented. Artificial Bee Colony (ABC) can be used to segment [5] the pre-processed image which is illustrated in [Figure 5].

Several methods, such as K-means, FCM and Ant Colony algorithms, are used for segmenting the Alzheimer disease nodules. FCM has a lengthy computing time and also sensitive to Speed, local minima and noise. It is challenging for K-means algorithms to estimate the number of clusters. The probability distribution varies each iteration in the Ant Colony approach and it is independent of the previous choice to select the optimum solution and also takes great deal of time for uncertain convergence. ABC overcomes these disadvantages. ABC is simple, sturdy and adaptable. It's simple to implement. It has less control settings for exploring local solutions and managing objective costs.

ABC segmentation has two important functions which are

$$PV_i = \frac{FV_i}{\sum_{m=1}^{SN} FV_i}$$

$$C_{ij} = I_{ij} + \emptyset_{ij} (I_{ij} - I_{kj}) \quad (5)$$

Where PV_i= probability value associated with i^{th} food source. A spectator bee chooses a food source that is based on PV_i

FV_i= i^{th} quantities of nectar of the food source measured by bees.

SN = No. of food sources equal to the number of bees employed. Fitness is calculated below by Eqn. (6).

$$FV_i = \{\frac{1}{(1+C_{ij}),\ C_{ij}\geq 0} 1 + abs(C_{ij}),\ C_{ij} < 0 \quad (6)$$

Where C_{ij} is the cost function.

3.3 Feature Extraction

The feature extraction step in Alzheimer classification is crucial for several reasons. Segmented Alzheimer image represent important characteristics of brain images. Feature extraction step aims to identify features that are highly discriminative for differentiating Alzheimer regions, structures, or pathological conditions, enabling efficient classification. There are several types of feature extraction methods commonly used in Alzheimer image classification. Each type serves a specific purpose and offers unique advantages. Intensity- based features capture statistical characteristics of the pixel intensities within Alzheimer images. These features provide information about the intensity distribution and textural patterns within brain regions, helping to differentiate different tissue types. Shape-based features describe the geometric properties of Alzheimer regions or structures. Shape-based features capture anatomical differences, structural abnormalities, or morphological changes associated with Alzheimer diseases. Texture-based features describe spatial patterns and relationships within Alzheimer images. Texture-based features [Table 1] which can be indicative of specific brain conditions or abnormalities.

3.3.1. LBP features

The LBP is one of feature extractor. It is used to extract texture feature by comparing each pixel with its neighbor. The neighbor window size varies from 1 to n. Finally, compared values are encoded as a bit.

3.3.2 Intensity features

As the mainly significant basis of image feature in Alzheimer images, color value feature is often utilized. [Table 2] describes the intensity characteristics and associated equation descriptions in more detail. The HOG feature is also evaluated while extracting the intensity feature.

3.3.3. Volumetric features

The Zernike moments describe gathering shapes in retrieving elements. At this time, the segmented image is first exposed to histogram equalization, which makes the bulk image boundaries further apparent.

SIFT characteristics are used since they are invariant for minor changes of light, size changes, rotation of the image and change of viewpoint.

3.3.4. Geometric features

3.3.4.1. Eccentricity

Eccentricity is termed in the following equation,

$$ECC = \sqrt{1 - \frac{x^2}{y^2}} \quad (7)$$

where x - Semi-major axis length of image ROI

y - Semi-minor axis length of image

3.3.4.2. Curvature descriptor

In terms of intensity, the curvature descriptor is calculated in the image area of interest that is dependent on the intensity fluctuation.

$$Cdd = tan^{-1}\left(\frac{\sqrt{\alpha_{1+}^2\alpha_2^2}}{1+f(x,y)}\right) \quad (8)$$

Where $\alpha_1$and α_2- two Eigen values of Hessian matrix (α_1 α_2).

3.4. Feature Selection

Feature selection is an essential step in the brain image classification process. It involves selecting a subset of relevant features from the original feature set to improve classification performance. Artificial Bee Colony (ABC) algorithm can be effective for feature selection. The ABC algorithm relies on the exploration and exploitation abilities of the bee colony to search for optimal

solutions. However, in feature selection problems with a large search space, the ABC algorithm may struggle to effectively explore the entire space and find the global optimal solution. This limitation can result in sub optimal feature subsets and hinder the algorithm's ability to discover the most informative features. The ABC algorithm often exhibits a slower convergence rate. The slower convergence can increase the computational time required to find an optimal feature subset. To overcome these drawbacks the output of ABC is given as input to the Pulse Coupled Neural Network (PCNN). PCNN does not require complex weight optimization or back propagation, making it computationally efficient and suitable for feature selection process. The parallel processing capability of the PCNN can enhance its performance in feature selection process [11].

Several current algorithms such as DE, GA, PSO are available for the feature selection process. GA does not ensure an optimum solution. This issue is addressed via the use of PSO. Both GA and DE are expensive to compute. But PSO is less costly computationally. In PSO, the best particle in each neighborhood influences other neighborhood particles. In order to address these issues, many particles in each neighborhood may affect others to a degree via a fluid variable. [Figure 6] explains the block diagram of BeePCNN feature selection algorithm. [Table 3] shown the performance of BeePCNN algorithm comparatively better than others.

3.5. Classification

The pooling layer in a convolutional neural network (CNN) is commonly used to down sample the feature maps, reducing their spatial dimensions while preserving important features. It plays a crucial role in capturing local invariance and reducing the computational complexity of subsequent layers. The Genetic Swarm Particle Optimization (GSPO) method combines the principles of genetic algorithms (GA) and particle swarm optimization (PSO) to enhance the search capabilities and convergence speed of optimization algorithms. The Genetic Swarm Particle Optimization (GSPO) method combines [9] the exploration capabilities of genetic algorithms (GA) with the exploitation abilities of particle swarm optimization (PSO). This combination leads to enhanced exploration and exploitation, accelerated convergence, and improved solution quality, making GSPO a powerful optimization technique [10]. The combination of Fuzzy genetic and PCNN is proposed as FGPCNN to perform classification which is given in [Figure 7]

4 . Results and Discussions

4.1. Data set used

In this work, we used a subset of the Alzheimer's Disease Neuroimaging Initiative (ADNI) data, which may be accessed and retrieved from their database at http://www.loni.ucla.edu/ADNI. The collection includes clinical data for thousands of patients as well as data from numerous imaging modalities, such as PET, functional MRI, MRI, genetic data, and MRI. We employed 160 subjects; MRI scans for our research. This dataset contains 52 NC, 62 MCI, and 46 AD patient's images.

4.1.1. Parameter setting

In our tests, we used two-dimensional FPSOs, D = 10 and D = 30. The number of repetitions was chosen at 1000 and 2000, respectively, to match the FPSO sizes of 10 and 30. In all tests, the number of particles was 30 and the number of experiments was 30. [Table 4] shows the parameters used in the ABC classification method, while [Table 5] shows the parameters used in the proposed CNN training and testing procedure.

4.2. Experimental Analysis

4.2.1. Analysis of Segmentation Approaches

The contribution of each classification method was evaluated in this experiment. K-Means, FCM, Ant Colony, and ABC are the classification techniques used for the study. An implementation parameter called overlap measurement is used to evaluate the effectiveness of this classification method. Ideally, a successful division method should have a large overlap. Overlapping measurements of classification methods such as K-means, FCM, Ant colony and ABC are listed in [Table 6].

The average value of the overlap produced by the ABC classification technique, as shown in [Table 6] is 0.933, which is higher than other current division methods. In

addition to the ABC classification technique, the Ant colony algorithm provides 0.913 for an effective D1 result. ABC received a score of 0.923 for D5, which is higher than other techniques.

4.2.2. Analysis of Feature Extraction Approaches

The contribution of each of the trait extraction methods used in this study was evaluated in this experiment. Efficiency indicators such as accuracy, sensitivity, precision and error rate are used to evaluate the performance of various functional search methods. Ideally, successful extraction methods should have high accuracy, high sensitivity, high accuracy and low error rate. [Table 7] shows the accuracy, precision, accuracy, and error measurement of various extraction methods. The proposed technique results in excellent accuracy, sensitivity, precision and error rates for D1 to D5.

In [Table 7] data set D1 gives more accuracy 97.47 % than individual download techniques for the proposed features. In addition, the error rate for D1, which is lower than the normal operation extraction technique, is 2.53 in the proposed output method. For D5, the accuracy achieved was 97.173, the sensitivity was 97.813, the specificity 97.473 and the error rate was 2.827.

4.2.3. Analysis of Classifier Approaches

In this experiment, the contribution of several classifications used in this study was evaluated. The performance criteria used to evaluate these

ratings are accuracy, precision, accuracy, and error rate [12]. Ideally, successful classifiers are expected to have high accuracy, high sensitivity, high accuracy, and low error rates. [Table 8] shows the accuracy, precision, accuracy, and error measurement of the various classifications.

Accuracy, sensitivity, error rates and accuracy for the five data sets are given as shown in [Table 8]. The proposed technique for D1 is 99.23, the sensitivity value is 99.31, and the output value is the specific value and the error rate is 0.77. The performance for D5 is 99.16 accuracy, 99.31 sensitivity with 99.18 accuracy and 0.84 error.

4.2.4 different optimization algorithms comparison with Bee and check the performance of the entire methodology

Table 9 : BeePCNN algorithm comparison with different optimization algorithms

Iteration	**Feature Selection Approaches**			
	Crow Search	**Butterfly**	**Giraffe Kick**	**BeePCNN**
1	110	103	98	94
2	136	126	121	122
3	154	145	140	140
4	159	154	149	145
5	163	155	150	150

Parameters used	Average Accuracy (%)	Average Error Rate (%)
Fourozannezhad et al. [35]	69.5	30.05
Hao et al. [36]	73.6	26.4
Shao et al. [44]	75.5	24.50
Modupe et al. [35]	94.32	5.68
Proposed	98.94	1.06

Table 10: Analysis of Proposed Method with Existing Deep Learning Approaches

4.2.5 Advantages and disadvantages

Advantages:

Detecting Alzheimer's disease from MRI images using Fuzzy Genetic Pulse Coupled Neural Network (FGPCNN) offers several advantages:

1. Early Detection: FGPCNN can identify subtle patterns and abnormalities in MRI scans that may not be obvious to human observers. This enables early detection

of Alzheimer's disease before symptoms become severe, allowing for earlier intervention and potentially better management of the condition.

2. Accuracy: FGPCNN architectures, coupled with advancements in training techniques such as Fuzzy Genetic Pulse Coupled Neural Network, can lead to higher accuracy in Alzheimer's detection. This means fewer false positives and false negatives, reducing the chances of misdiagnosis.

3. Automation: Once trained, FGPCNN models can automate the process of analyzing MRI scans for signs of Alzheimer's disease. This can significantly reduce the workload on radiologists and clinicians, allowing them to focus on more complex cases and patient care.

4. Scalability: FGPCNN -based approaches can be easily scaled to handle large volumes of MRI data, making them suitable for population-wide screening programs or large-scale clinical studies aimed at understanding Alzheimer's disease progression.

5. Objective Evaluation: FGPCNN models provide an objective and consistent way to evaluate MRI scans for Alzheimer's-related biomarkers. This reduces the potential for variability in interpretation that can occur with human observers and reduce the cost.

6. Feature Extraction: FGPCNN can automatically learn relevant features from MRI images without the need for manual feature engineering. This is particularly advantageous in medical imaging, where relevant features may be complex and difficult to define.

Disadvantages:

1. Data Availability and Quality: Access to large, high-quality labeled MRI datasets for training CNN models can be limited, especially considering the need for diverse datasets that capture various stages and manifestations of Alzheimer's disease. Biases in the training data can lead to model inaccuracies and generalization issues.

2. Generalization to Clinical Practice: While FGPCNN models may perform well in controlled research settings, their performance in real-world clinical practice may vary due to differences in patient demographics, scanner variability, and imaging protocols. Robust evaluation and validation in diverse clinical settings are necessary to ensure the reliability of CNN-based Alzheimer's detection systems.

Computational Complexity

The computational complexity of CNN is calculated by using big o notation. The computational complexity of CNN is calculated using Eq. (32)

$$\text{CNN Time Complexity} = n_{layers} \text{ . Convolution filer size. Pooling size} \quad (32)$$

$$\text{CNN} = O(n^2 . n^4 . n^2) = O(n^8) \quad (33)$$

The computational complexity of PSOCNN is found by using Eq. (34)

$$\text{PSOCNN (Particle Swarm Optimization CNN) Time Complexity} = n_{layers} \text{ . Convolution filer size} \quad (34)$$

$$\text{PSOCNN} = O(n^1 . n^4) = O(n^5) \quad (35)$$

The computational complexity of GACNN is found by using Eq. (36)

$$\text{GACNN (Genetic Algorithm CNN) Time Complexity} = n_{layers} \text{ . Convolution filer size} \quad (36)$$

$$\text{GACNN} = O(n^1 . n^4) = O(n^5) \quad (37)$$

The computational complexity of FGPSOCNN is found by using Eq. (38)

$$\text{FGPCNN (Fuzzy Genetic PCNN) Time Complexity} = n_{layers} \text{ . Convolution filer size} \quad (38)$$

$$\text{FGPCNN} = O(n^1 . n^4) = O(n^5) \quad (39)$$

Conflict of interest (COI)

We declare that we have no conflict of interest in the publication.

References

[1] Mehmood A, Maqsood M, Bashir M, Shuyuan Y. A Deep Siamese Convolution Neural Network for Multi-Class Classification of Alzheimer Disease. Brain Sci. 2020 Feb 5;10(2):84. doi: 10.3390/brainsci10020084. PMID: 32033462; PMCID: PMC7071616.

[2] Stevenson, Jenna, Nesrine Rahmouni, Mira Chamoun, Andréa Lessa Benedet, Alyssa Stevenson, Vanessa Pallen, Joseph Therriault et al. "TRIAD multi-dimensional biobank for biomarker discovery." Alzheimer's & Dementia 18 (2022): e067980.

[3] Zhang, B. and Allebach, J.P., 2008. Adaptive bilateral filter for sharpness enhancement and noise removal. IEEE transactions on Image Processing, 17(5), pp.664-678.

[4] Masouleh, M.K. and Shah-Hosseini, R., 2018. Fusion of deep learning with adaptive bilateral filter for building outline extraction from remote sensing imagery. Journal of Applied Remote Sensing, 12(4), pp.046018-046018.

[5] Xiao, S., Wang, W., Wang, H. and Huang, Z., 2022. A new multi- objective artificial bee colony algorithm based on reference point and opposi- tion.

International Journal of Bio-Inspired Computation, 19(1), pp.18-28.

[6] Zhou, M., Ng, M., Cai, Z. and Cheung, K.C., 2020. Self-attention-based fully inception networks for continuous sign language recognition. In ECAI 2020 (pp. 2832-2839). IOS Press.

[7] Basheera, S. and Ram, M.S.S., 2019. Convolution neural network-based Alzheimer's disease classification using hybrid enhanced independent component analysis based segmented gray matter of T2 weighted magnetic resonance imaging with clinical valuation. Alzheimer's & Dementia: Translational Research & Clinical Interventions, 5, pp.974-986.

[8] Basheera, S. and Ram, M.S.S., 2021. Deep learning-based Alzheimer's disease early diagnosis using T2w segmented gray matter MRI. International Journal of Imaging Systems and Technology, 31(3), pp.1692-1710.

[9] Alrefai, N. and Ibrahim, O., 2022. Optimized feature selection method using particle swarm intelligence with ensemble learning for cancer classification based on microarray datasets. Neural Computing and Applications, 34(16), pp.13513-13528.

[10] Dabba, A., Tari, A. and Meftali, S., 2023. A new multi objective binary Harris Hawks optimization for gene selection in microarray data. Journal of Ambient Intelligence and Humanized Computing, 14(4), pp.3157-3176.

[11] Basar, S., Waheed, A., Ali, M., Zahid, S., Zareei, M. and Biswal, R.R., 2022. An efficient defocus blur segmentation scheme based on Hybrid LTP and PCNN. Sensors, 22(7), p.2724.

[12] Indhumathi, R. and Narmadha, T.V., 2022. Hybrid pixel based method for multimodal image fusion based on Integration of Pulse Coupled Neural Network (PCNN) and Genetic Algorithm (GA) using Empirical Mode Decomposition (EMD). Microprocessors and Microsystems, 94, p.104665.

[13] Beatrice, S., and Janaki Meena. "Overhauled Approach to Effectuate the Amelioration in EEG Analysis." Intelligent Automation Soft Computing 33, no. 1 (2022).

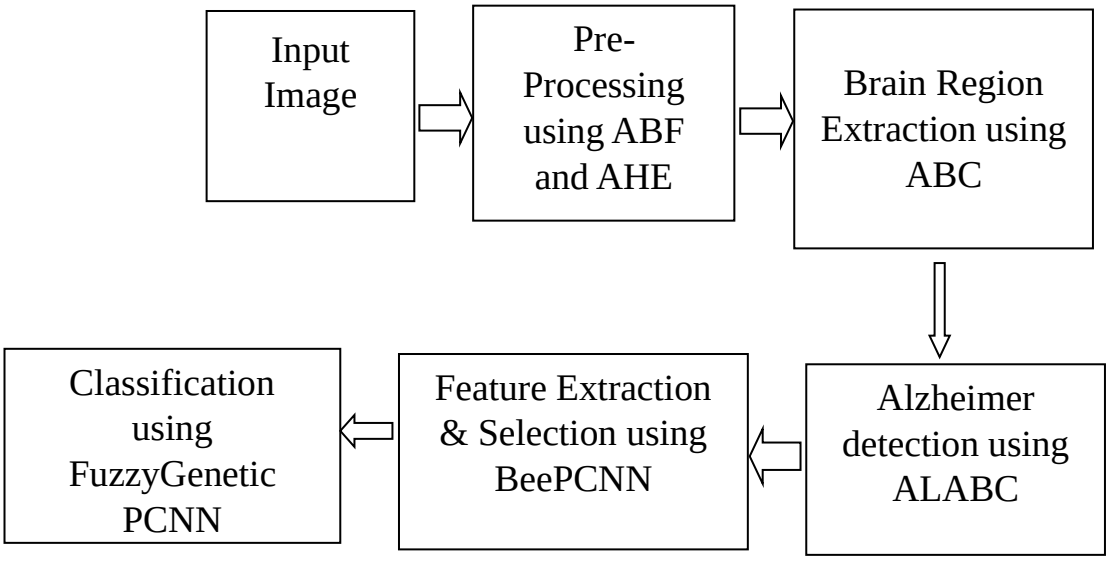

.

Fig 1. Flow of the proposed work

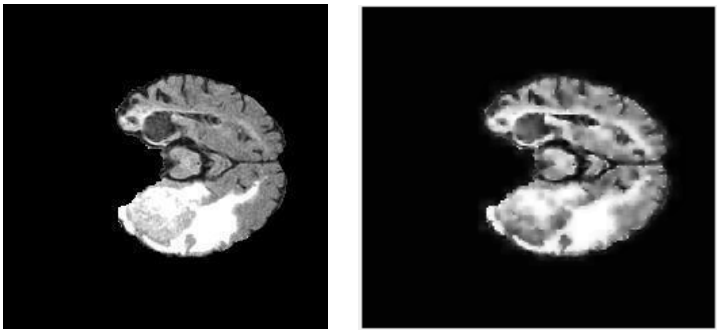

(a) (b)

Fig. 2. (a). Input Alzheimer image, 2(b). histogram equalized image

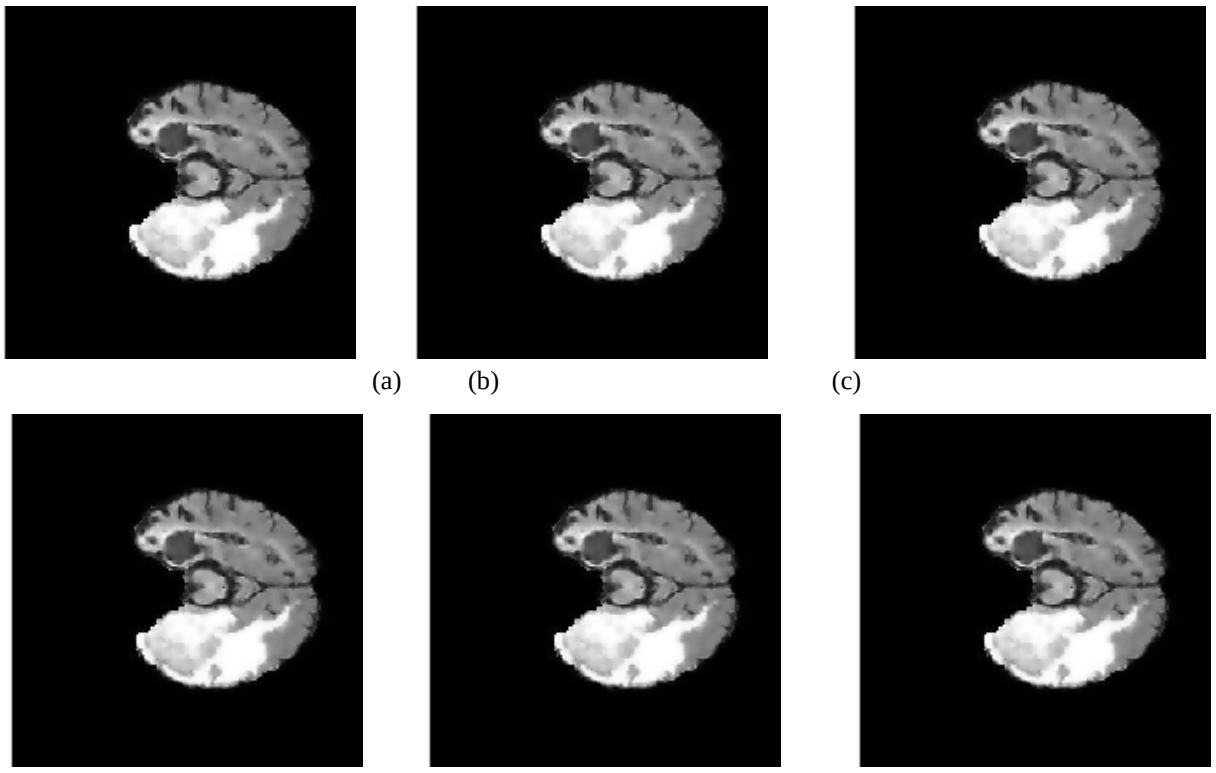

(a) (b) (c)

(d) (e) (f)

Fig 3. Result of $\nabla_r \; and \; \nabla_{d.}$ 4.(a). $\nabla_d = 1$, 4.(b). $\nabla_r = 1$, 4.(c). $\nabla_r = 5$, 4.

(d). $\nabla_r = 10$, 4. (e). $\nabla_r = 25$, 4.(f). $\nabla_r = 50$

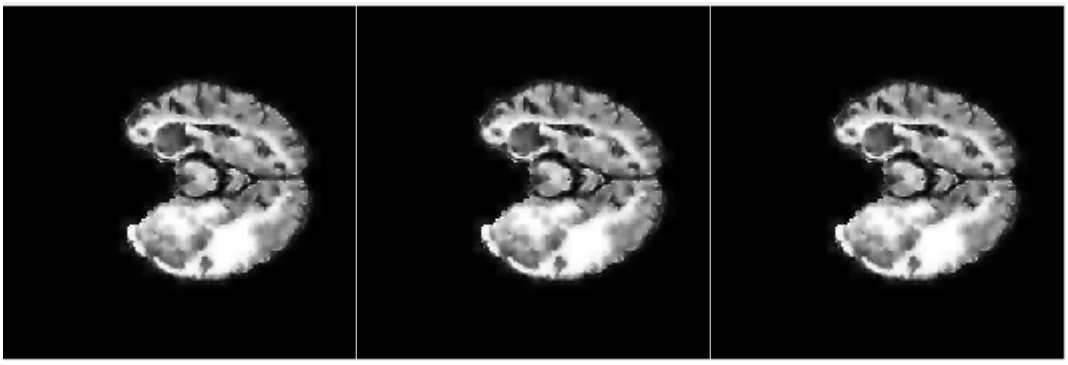

(a) (b) (c)

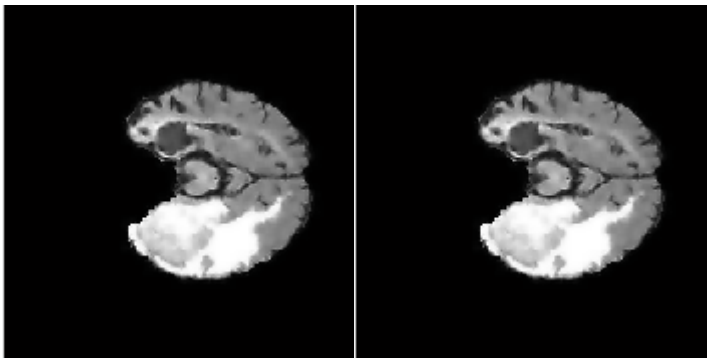

(d) (e)

Fig 4(a).Input, 4(b).Mean filtered image, 4(c).Median filtered image, 4(d).Bilateral filtered image and 4(e). ABF filtered image

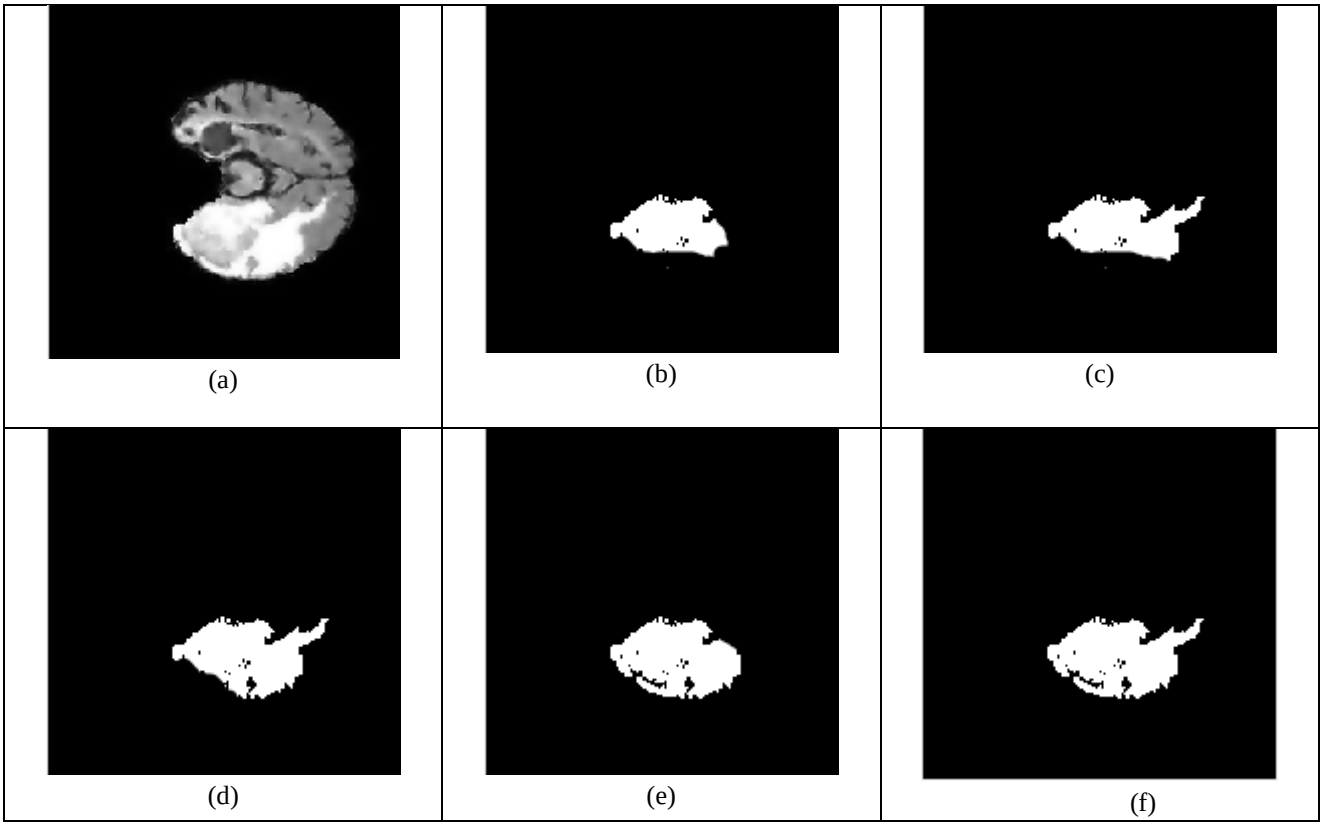

(a) (b) (c)

(d) (e) (f)

Fig 5(a). Input image 5(b). Pre-processed image 5(c). Segmentation using k-means, 5(d). FCM Result 5(e). Ant colony Result, 5(f). ABC Result

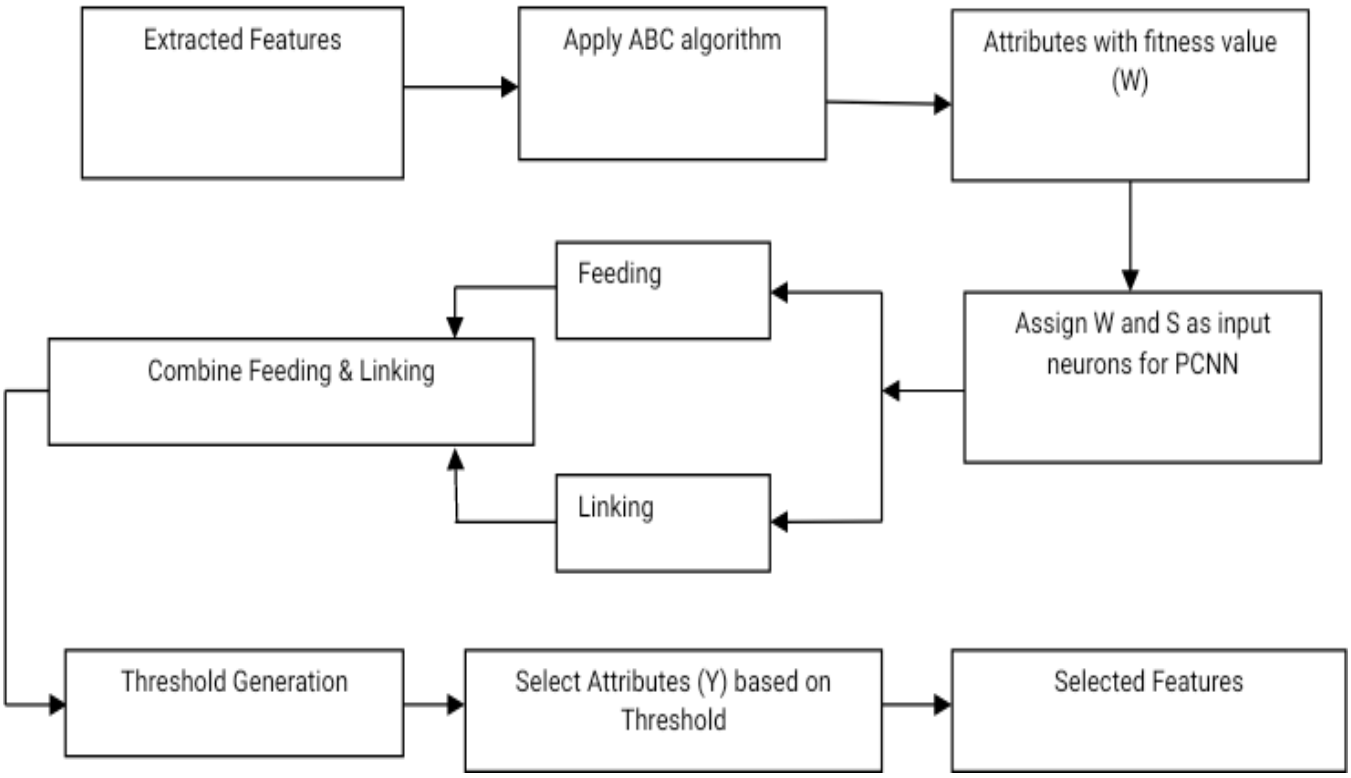

Fig. 6. Feature Selection (BeePCNN) Algorithm

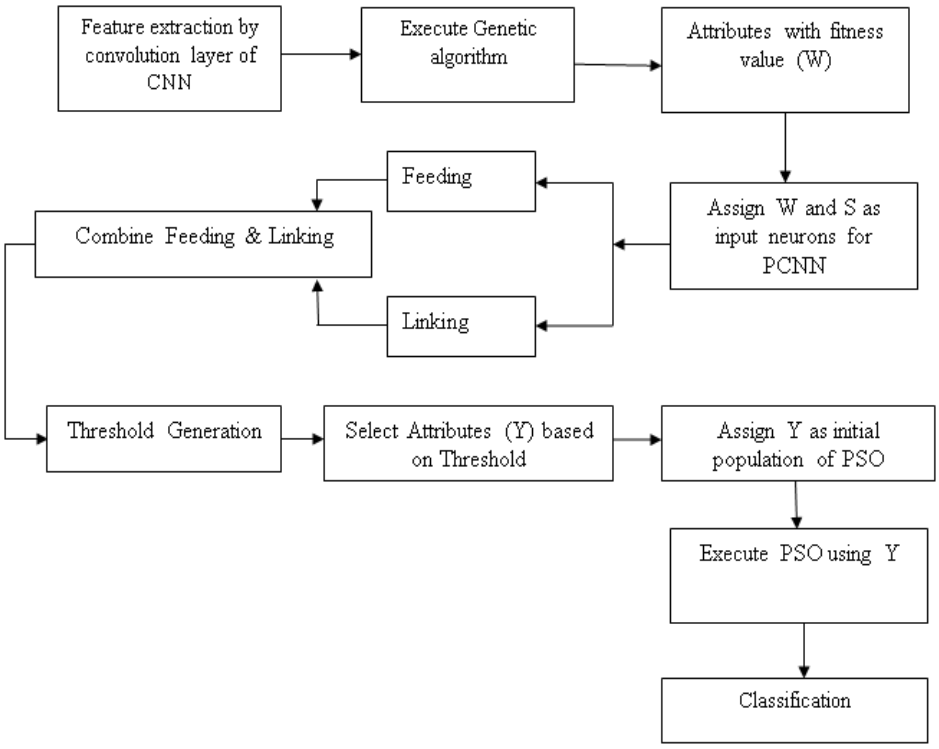

Fig 7. Outline of the Proposed Classifier FGPCNN Algorithm

Texture features used	Equation
Variance	$\sum_{k=0}^{l-1} k^2 P_{x-y}(k)$
Sum average	$\sum_{k=0}^{l-1} k^2 P_{x+y}(k)$
Maximum probability	$max_{i,j}\, X(i,j)$
Contrast	$\sum_{i=0}^{l-1}\sum_{j=0}^{l-1} \lvert i-j\rvert^2\, X(i,j)$
Auto-correlation	$\sum_{i=0}^{l-1}\sum_{j=0}^{l-1} \lvert i-j\rvert\, X(i,j)$

Table 1. Retrieved Texture features

Intensity features used	Equation with description
Mean	$\frac{1}{P^2}\sum_{k=1}^{P}\sum_{l=0}^{P} I_{(k,l)}$
Standard Deviation σ	$\sqrt{\frac{1}{P}\sum_{k=0}^{P} I_k - \underline{x}^2}$
Skewness	$\frac{\sum_{k=0}^{PP}(I_k-x)^3}{(P-1)\sigma^2}$
Entropy	$\frac{1}{2}\left(\sum_{k=0}^{255}\sum_{l=0}^{255} G_H(k,l).log\,(G_H(k,l)) + \sum_{k=0}^{255}\sum_{l=0}^{255} G_V(k.l).log(G_V(k,l))\right)$
Max-Intensity	Max[I(k,l)]

Table 2. Intensity features

Iteration	Feature Selection Approaches			
	ABC	**FPSO**	**PCNN**	**BeePCNN**
1	115	108	99	94
2	141	131	127	122
3	159	150	144	140
4	164	159	151	145
5	168	160	155	150

Table 3. Analysis of Feature Selection Approaches

Parameters	Values
Size of bees	100
Max Iteration	5000
No of Employee Bees	50
No of Onlooker Bees	49
No of Scouts	1

Table 4. Parameters and its values of ABC

Parameters	Values
Total Layers	3
Total input layer	8
Total Hidden Layers	10, ….50
Total Output Layers	1
AF	Radial Basis
SSE value	1

Table 5. Parameters and its values of proposed CNN

Data sets	Segmentation Approaches			
	K-Means	FCM	Ant Colony	ABC
D1	0.805	0.884	0.913	**0.933**
D2	0.821	0.9	0.929	**0.949**
D3	0.832	0.911	0.94	**0.96**
D4	0.85	0.929	0.958	**0.978**
D5	0.795	0.874	0.903	**0.923**

Table 6. Overlap measures Analysis of K-Mean, FCM, Ant Colony and ABC

Metrics	Acc	Sen	Spec	Error
	D1			
Intensity	82.23	91.13	94.35	17.77
HOG	83.14	92.15	93.52	16.86
Wavelet	83.66	90.74	94.74	16.34
LBP	82.58	91.4	93.91	17.42
SIFT	81.12	90.51	92.85	18.88
Zernike	82.71	89.82	93.8	17.29
Eccentricity	81.6	90.53	92.62	18.4
Curvature	80.28	89.64	91.28	19.72
Proposed	**97.47**	**98.11**	**97.77**	**2.53**
	D2			
Intensity	82.252	91.152	94.372	17.792
HOG	83.162	92.172	93.542	16.882
Wavelet	83.682	90.762	94.762	16.362
LBP	82.602	91.422	93.932	17.442
SIFT	81.142	90.532	92.872	18.902
Zernike	82.732	89.842	93.822	17.312

Eccentricity	81.622	90.552	92.642	18.422
Curvature	80.302	89.662	91.302	19.742
Proposed	**97.492**	**98.132**	**97.792**	**2.552**
	D3			
Intensity	82.033	90.933	94.153	17.967
HOG	82.943	91.953	93.323	17.057
Wavelet	83.463	90.543	94.543	16.537
LBP	82.383	91.203	93.713	17.617
SIFT	80.923	90.313	92.653	19.077
Zernike	82.513	89.623	93.603	17.487
Eccentricity	81.403	90.333	92.423	18.597
Curvature	80.083	89.443	91.083	19.917
Proposed	**97.273**	**97.913**	**97.573**	**2.727**
	D4			
Intensity	81.623	90.523	93.743	18.377
HOG	82.533	91.543	92.913	17.467
Wavelet	83.053	90.133	94.133	16.947
LBP	81.973	90.793	93.303	18.027
SIFT	80.513	89.903	92.243	19.487
Zernike	82.103	89.213	93.193	17.897
Eccentricity	80.993	89.923	92.013	19.007
Curvature	79.673	89.033	90.673	20.327
Proposed	**96.863**	**97.503**	**97.163**	**3.137**
	D5			
Intensity	81.933	90.833	94.053	18.067
HOG	82.843	91.853	93.223	17.157
Wavelet	83.363	90.443	94.443	16.637
LBP	82.283	91.103	93.613	17.717
SIFT	80.823	90.213	92.553	19.177
Zernike	82.413	89.523	93.503	17.587
Eccentricity	81.303	90.233	92.323	18.697
Curvature	79.983	89.343	90.983	20.017
Proposed	**97.173**	**97.813**	**97.473**	**2.827**

Table 7. Performance Analysis of Feature Extractor on Real-time Dataset

Metrics	**Acc**	**Sen**	**Spec**	**Error**
	D1			
SVM	94.23	95.61	94.91	5.77
Bagging	89.26	90.75	89.95	10.74
Naive Bayes	85.71	86.63	86.42	14.29
KNN	84.23	85.21	84.96	15.77
AdaBoost	91.76	92.82	92.43	8.24
ELM	97.14	98.39	97.87	2.86
CNN	98.18	98.43	98.76	1.82
GACNN	98.76	98.88	98.93	1.24
PSOCNN	98.91	98.95	98.99	1.09
FGPCNN	**99.23**	**99.31**	**99.43**	**0.77**
	D2			
SVM	94.272	95.652	94.952	5.728
Bagging	89.302	90.792	89.992	10.698
Naive Bayes	85.752	86.672	86.462	14.248

KNN	84.272	85.252	85.002	15.728
AdaBoost	91.802	92.862	92.472	8.198
ELM	97.182	98.432	97.912	2.818
CNN	98.2	98.45	98.78	1.8
GACNN	98.78	98.9	98.95	1.22
PSOCNN	98.93	98.97	99.01	1.07
FGPCNN	**99.12**	**99.23**	**99.35**	**0.88**
	D3			
SVM	94.161	94.971	94.841	5.839
Bagging	89.191	90.011	89.881	10.809
Naive Bayes	85.641	86.481	86.351	14.359
KNN	84.161	85.021	84.891	15.839
AdaBoost	91.691	92.491	92.361	8.309
ELM	97.071	97.931	97.801	2.929
CNN	98.05	98.76	98.63	1.95
GACNN	98.63	98.93	98.8	1.37
PSOCNN	98.78	98.99	98.86	1.22
FGPCNN	**99.18**	**99.33**	**99.2**	**0.82**
	D4			
SVM	94.121	94.931	94.801	5.879
Bagging	89.151	89.971	89.841	10.849
Naive Bayes	85.601	86.441	86.311	14.399
KNN	84.121	84.981	84.851	15.879
AdaBoost	91.651	92.451	92.321	8.349
ELM	97.031	97.891	97.761	2.969
CNN	98.01	98.72	98.59	1.99
GACNN	98.59	98.89	98.76	1.41
PSOCNN	98.74	98.95	98.82	1.26
FGPCNN	**99.14**	**99.29**	**99.16**	**0.86**
	D5			
SVM	94.121	94.931	94.801	5.879
Bagging	89.151	89.971	89.841	10.849
Naive Bayes	85.601	86.441	86.311	14.399
KNN	84.121	84.981	84.851	15.879
AdaBoost	91.651	92.451	92.321	8.349
ELM	97.031	97.891	97.761	2.969
CNN	98.01	98.72	98.59	1.99
GACNN	98.59	98.89	98.76	1.41
PSOCNN	98.74	98.95	98.82	1.26
FGPCNN	**99.14**	**99.29**	**99.16**	**0.86**

Table 8. Analysis of Classifiers on Real-time Dataset